34th Annual International Conference of the IEEE EMBS
San Diego, California USA, 28 August - 1 September, 2012

Mycobacterium Tuberculosis Recognition with Conventional Microscopy

Cicero F. F. CostaFilho, Pamela C. Levy, Clahildek M. Xavier, Marly G. F. Costa, Luciana B.M.Fujimoto, Julia Salem

Abstract— **This paper presents a new method for segmentation of tuberculosis bacillus in conventional sputum smear microscopy. The method comprises three main steps. In the first step, a scalar selection are made for characteristics from the following color spaces: RGB, HSI, YCbCr and Lab. The features used for pixel classification in the segmentation step were the components and subtraction of components of these color spaces. In the second step, a feedforward neural network pixel classifier, using selected characteristics as inputs, is applied to segment pixels that belong to bacilli from the background. In third step geometric characteristics, especially the eccentricity, and a new proposed color characteristic, the color ratio, are used to noise filtering. The best sensitivity achieved in bacilli detection was 91.5%.**

I. Introduction

According to the Global TB control report of 2010 by the World Health Organization-WHO [1], the global burden of disease caused by Tuberculosis - TB in 2009 is as follows: 9.4 million incident cases, 14 million prevalent cases, 1.3 million deaths among non HIV-positive individuals and 0.38 million deaths among HIV positive people.

To eradicate TB, the WHO adopted a Global Partnership Plan, launched in January 2006, which includes smear sputum microscopy as the main diagnostic tool.

Two techniques are used for TB diagnostic with sputum smear microscopy: Fluorescence microscopy and conventional microscopy. Fluorescence microscopy uses an acid-fast fluorochrome dye (e.g., auramine O or auramine-rhodamine), while conventional microscopy uses the carbolfuchsin Ziehl-Neelsen - ZN or Kinyoun acid-fast stains.

While the former uses an intense light source, such as a halogen or high-pressure mercury vapor lamp, the latter uses a conventional artificial light source.

Fluorescence microscopy has the following main advantages over conventional microscopy: 1) Fluorescence microscopy uses a lower power objective lens (typically 25x), while conventional microscopy uses a higher power objective lens (typically 100x). As a consequence, fluorescence microscopy allows the same area of a smear to be scanned in a much short timer than conventional microscopy [2];

2) Fluorescence microscopy is on average 10% more sensitive than conventional microscopy [3].

The main shortcomings of fluorescence microscopy are: 1) The relatively high costs of the microscopy unit and its maintenance compared with the conventional microscopy unit; 2) The handling and maintenance of the optical equipment require advanced technical skill [4].

TB diagnosis in sputum smear microscopy is performed by counting the number of bacilli present in approximately 100 fields. This counting can be done manually or automatically.

Some authors [5-7] claimed that the main advantages of an automatic bacilli screening over a manual one are better reproducible values for sensitivity and specificity and a faster screening process.

Steps involved in automated microscopy include those shown if Figure 1.

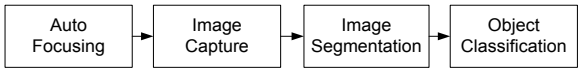

Fig. 1 Steps involved in bacilli segmentation

In fluorescence microscopy images, the bacilli are easily separated from the background with a threshold operation. Afterwards, the segmentation is performed using edge detection operators, such as canny operators (Veropoulos et. al., 1998; Forero et. al., 2004) [8-9]. Intermediate steps for edge linking and boundary tracing are also employed. In conventional microscopy images, the bacilli are not easily separated from the background with a threshold operation. In this case, for bacilli segmentation, color space techniques are used. The techniques found in the literature vary: histogram

C. F. F. Costa Filho is with *Universidade Federal do Amazonas/Centro de Pesquisa e Desenvolvimento em Tecnologia Eletrônica e da Informação* – UFAM/CETELI. Manaus. Amazonas. Brasil (tel:: +55 92 91464954; e-mail: cfffilho@gmail.com).

Pamela C. Levy is with *Universidade Federal do Amazonas/Centro de Pesquisa e Desenvolvimento em Tecnologia Eletrônica e da Informação* – UFAM/CETELI. Manaus. Amazonas. Brasil (tel: +55 92 8414 1406; e-mail: pamela.levy@gmail.com).

Clahildek M. Xavier is with *Universidade Federal do Amazonas/Centro de Pesquisa e Desenvolvimento em Tecnologia Eletrônica e da Informação* – UFAM/CETELI. Manaus. Amazonas. Brasil (tel: +55 92 8414 1406; e-mail: clahildek@gmail.com).

M. G. F. Costa is with *Universidade Federal do Amazonas/Centro de Pesquisa e Desenvolvimento em Tecnologia Eletrônica e da Informação* – UFAM/CETELI. Manaus. Amazonas. Brazil (tel: +55 92 9128 2404; e-mail: mcosta@ufam.edu.br).

L. B. M. Fujimoto is with *Instituto Nacional de Pesquisas da Amazônia - INPA*.Manaus. Amazonas. Brasil (tel: +55 92 9981 4649; e-mail: olfujimoto@vivax.com.br)

Julia Salem is with *Instituto Nacional de Pesquisas da Amazônia - INPA*.Manaus. Amazonas. Brasil (tel: +55 92 9981 4649; e-mail: julia.salem@inpa.gov.br)

based techniques, Bayesian pixel classifiers, KNN pixel classifiers, etc. The color spaces used also vary: RGB, YCbCr and Lab. The majority of the authors used the RGB color space. Only Sotaquirá et al. [6] used a combination of components of color spaces YCbCr and Lab.

This paper proposes a new method for bacilli segmentation in sputum smear microscopy. The main features of the proposed method that distinguish it from the others are:

1) It classifies the images according to the background content, as belonging to a group of high background density or to a group of a low background density.
2) The input variables for the segmentation classifier were selected from the components and subtraction of components of the following color spaces: RGB, HSI, YCbCr and Lab.
3) For bacilli classification, associated with geometric variables, a new parameter of color measure, called *color ratio*, was used

In the sequence, this new method is described.

II. Materials and Methods

A. Materials

A total of 120 images were used with a spatial resolution of 2816x2112 pixels, obtained from sputum smear microscopy slices of 12 patients. The samples were prepared using the Kinyoun acid-fast stain and counterstained with methylene blue solution. The images were captured using a digital camera model Canon Power Shot A640 of 10 megapixels, attached to a conventional microscope model Zeiss Axioskop 4 (second block of Fig.1).

The samples were prepared in Laboratory of the Instituto Nacional de Pesquisas da Amazonia (INPA), Manaus, Brazil. The image focus (first block of Fig.1) was established in a previous work of Kimura et al. [10].

B. Image Groups

For bacilli segmentation, based on the background content, the images were divided in two main groups: a) high density of background content (HDB) and b) low density of background content (LDB). The HDB group is characterized by a strong presence of counterstain with methylene blue solution in the background, while the LDB group is characterized by a weak presence of this same counterstain. Fig. 2 shows one image of the HDB type and other image of the LDB type. As shown, in the background of HDB images, there is a prevalence of the blue color, while in the background of LDB images there is a prevalence of white color.

For classification of the images in these two groups, the hue component of the HSI space was used. For each image, the percentage of pixels in the range of the blue color (0.5-0.7) was calculated. For each image, the percentage of pixels with a hue component in the blue color range was obtained. Fig. 3 shows this percentage, for images of both groups, represented with bars. The bars were organized so that the first 60 images have bars corresponding to low percentage values, and the last 60 images have bars corresponding to high percentage values. An experimental threshold of 13.56 was established to separate images as belonging to group LDB or to group HDB. This threshold value is shown as a horizontal line in Fig. 3. When the bar value was less than this threshold, the image was considered as belonging to the LDB group. When the bar value was higher than this threshold, the image was considered as belonging to the HDB group.

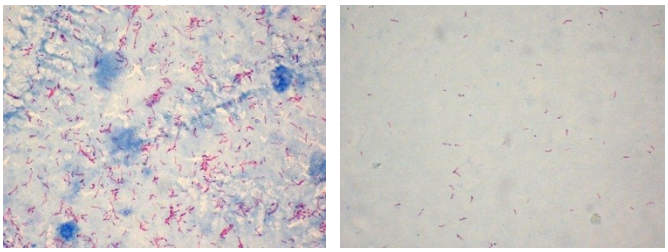

(a) (b)

Fig. 2 (a) Image with high density of background content; (b) Image with low density of background density.

C. Segmentation

The features used for pixel classification in the segmentation step were the components and subtraction of components of the following color spaces: RGB, HSI, YCbCr and Lab. A set, F, of 30 features was used: F = {R, G, B, R-B, R-G, G-B, ~R, ~G, ~B, H, S, I, H-S, H-I, S-I, R-I, G-I, B-I, Y, Cb, Cr, Y-Cb, Y-Cr, Cb-Cr, L, a, b, L-a, L-b, a-b}. The technique used to select the best features was scalar feature selection one [11]. For application of this technique, from each of the 120 images, 20 pixels belonging to bacilli and 20 pixels belonging to the background were extracted. Sets with 4,5,6,7 and 8 features were produced as a result. Table I shows the selected feature (selection done with scalar feature selection technique) of each one of these sets.

A classification method employing a neural network (NN) was used. The training of the classifiers was done using 1200 pixels belonging to bacilli and 1200 pixels belonging to the background. The test set was also comprised of 1200 pixels belonging to the bacilli and 1200 pixels belonging to the background. These pixels were extracted from all 120 images.

The NN used had an *n-m-1* architecture. To adjust the best architecture, the values of *n* and *m* assumed values of the following set: {3,6,0,12,15,19}. A total of 180 simulations were done combining different values of *n* and *m*. The training algorithm used was the backpropagation one associated with the Levenberg-Marquardt optimization method [12]. The convergence criteria used was a quadratic error of 10^{-4}.

D. Classification

For bacilli classification a combination of geometric characteristics and a parameter called *color ratio* was used. The following geometric characteristics were investigated: area, perimeter, compactness, eccentricity and the Hu´s moments of the first, second and third order:

$\mu_{10}, \mu_{02}, \mu_{20}, \mu_{11}, \mu_{12}, \mu_{21}, \mu_{30}, \mu_{03}$. The idea was to select one of the best geometric characteristics to classify bacilli. For this purpose, the contours of 500 bacilli were extracted [13] and the following parameters were calculated for each one of these geometric characteristics: average value (η), standard deviation (σ) and variation coefficient (v), defined as:

$$v = \frac{\sigma}{\eta}.100 \quad (1)$$

The best geometric characteristic chosen was the one with the lowest value of v. Table II shows these parameter values. As shown, the best geometric characteristic determined was the eccentricity. In order to minimize the false positive value in classification, a threshold value of 0.77 was used for the eccentricity for bacilli and noise classification. Objects with eccentricity higher than 0.77 were considered bacilli; otherwise, they were considered noise.

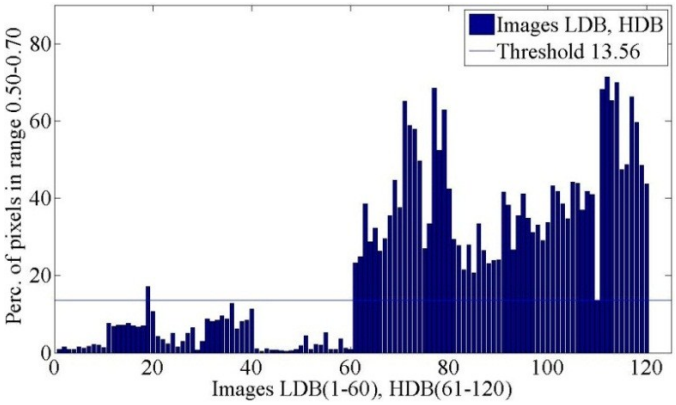

Fig. 3 Bar percentages for all images of groups LDB and HDB.

For images of group 1 the eccentricity was enough to obtain good classification rates. For images of group 2, nevertheless, another parameter, the *Color Ratio (CR)* was employed. This parameter is defined with the aid of Fig. 4. Two points are initially defined as C_p and B_p. The first one corresponds to the center of bacillus. The second one is the first point out of a bacillus, on the same horizontal axis, on the left or right side of the center point, if the bacillus major axis is vertical. If the bacillus major axis is horizontal, the second point is the first point out of bacillus, on the same vertical axis, on the up or down side of center point. Fig.4 shows a bacillus with vertical major axis and B_p was chosen on the left side of the center point C_p (it also could be on right side).

TABLE I
SETS OF SELECTED FEATURES FOR PIXEL CLASSIFICTION

Number of features	Sets of selected features
4	*G-I, L-a, Y-Cr, a*
5	*G-I, L-a, Y-Cr, a, R-G*
6	*G-I, L-a, Y-Cr, a, R-G, H-I*
7	*G-I, L-a, Y-Cr, a, R-G, H-I, a-b*
8	*G-I, L-a, Y-Cr, a, R-G, H-I, a-b, H*

For the definition of *CR* in expression (4), the intensity differences of red and green components on the center point and border point was used, as defined in expression (2) and (3):

TABLE II
GEOMETRIC CHARACTERISTICS PARAMETERS

Parameter / Geometric Characteristic	Average Value	Standard Deviation	Variation Coefficient
Area	625.34	232.09	37.12
Perimeter	126.03	34.08	27.04
Eccentricity	0.95	0.03	2.96
Compactness	0.51	0.12	23.11
μ_{10}	1.06	0.27	25.31
μ_{02}	24.47	0.73	29.46
μ_{20}	7.61	1.39	18.32
μ_{11}	8.73	1.17	13.38
μ_{12}	17.60	2.06	11.68
μ_{21}	5.23	1.27	24.34
μ_{22}	17.66	2.23	12.61

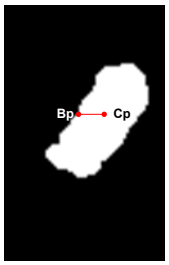

Fig. 4 This figure was used to define the color ratio. Cp – bacillus center point, Bp– bacillus border point.

$$dif_R = R_{C_p} - R_{B_p} \quad (2)$$

$$dif_G = G_{C_p} - G_{B_p} \quad (3)$$

$$CR = \frac{dif_R}{dif_G} \quad (4)$$

Where: R_{C_p} - value of Red component in C_p,
R_{B_p} - value of Red component in B_p.
G_{C_p} - value of Green component in C_p
G_{B_p} - value of Green component in B_p

The idea explored with the *CR* filter is the following. Due to the Kinyoun acid-fast stain, when bacillus is over a white background (with a weak presence of counterstain with methylene blue solution), its color is light fuchsia. When the bacillus is over a blue background (with the strong presence of a counterstain with methylene blue solution), its color is dark purple. In the first case, there is a predominance of the red component over the green and blue components. In the second case there is a predominance of the blue component over the other two components. The red component, nevertheless, is predominant over the green component. These observations are summarized in the rules just presented.

To demonstrate the application of these rules, we use the following figures: Fig. 5(a) shows an original group 2 image,

Fig 5(b) shows the output of segmentation; Fig. 5(c) shows the output of the eccentricity filter and Fig 5(d) shows the output of the *color ratio* filter. Fig. 5(b) shows four marked objects: O_1 and O_2 – these objects are not bacilli and are eliminated with an eccentricity filter. Objects O_3 and O_4 – these objects are not bacilli and are eliminated only with the *CR* filter; O_5 – is a bacillus, not eliminated in both filters. Fig 6(a), Fig 6(b) and Fig 6(c) show a profile of component intensity of objects O_3, O_4 and O_5. In each graph, the coordinate $x = 0$ corresponds to point B_p and the right coordinate of the graph, to C_p. Table III shows values of dif_R, dif_G and CR for objects O_3 and O_4.

The following set or rules, *color ratio* filter, are used to decide if an object is a bacillus or noise:

$$
\begin{aligned}
&if\ R_{C_p} > G_{C_p}\ and\ R_{C_p} > B_{C_p}\\
&\quad object\ is\ bacillus\\
&elseif\ \ R_{C_p} > G_{C_p} and\ R_{C_p} < B_{C_p}\\
&\quad if\ dif_R > 0\ and\ dif_G > 0\ and\ CR > 2\\
&\quad\quad object\ is\ a\ bacillus\\
&\quad elseif\ dif_R > 0\ nd\ dif_G < 0\\
&\quad\quad object\ is\ a\ bacillus\\
&\quad elseif\ dif_R < 0\ and\ dif_G < 0\ and\ CR < 0.5\\
&\quad\quad object\ is\ a\ bacillus\\
&\quad else\\
&\quad\quad object\ is\ not\ a\ bacillus\\
&elseif\ R_{C_p} < G_{C_p}\ and\ R_{C_p} < B_{C_p}\\
&\quad object\ is\ not\ a\ bacillus\\
&end
\end{aligned}
$$

Where: B_{C_p} - value of Blue component in C_p

TABLE III
VALUES OF DIF_R, DIF_G AND CR FOR OBJECTS O_3 AND O_4

Object	Characteristic		
	dif_R	dif_G	CR
O_3	-65	-85	0.76
O_4	-62	-86	0.72

III. RESULTS

First, we will comment on the segmentation results. The best accuracy of the neural network used to pixel classification was obtained with architecture 18-3-1 and with the set of 5 selected features. The ground truth for training and testing the neural network are the sets of pixels extracted from bacilli and from background.

Table IV shows the values of accuracy, sensitivity and specificity of the best pixel classifier.

Table V shows the results of the best classifier applied to bacilli classification using all 120 images. In all these images the ground truth was established by a physician that marked all bacilli and noise objects. The precision is defined as the ratio of quantity of bacilli correctly classified and number of objects classified as bacilli. False detection is defined as the ratio of the quantity of noise classified as bacilli and number of objects classified as bacilli. The ground truth for object classification as bacillus or noise is

Table VI shows the result after eccentricity filter application, while Table VII shows the result after CR filter application.

IV. CONCLUSION

A new technique for bacilli recognition was presented in this paper. The main difference of this paper from others previously presented is that the features used as input of classifiers were selected from four different space colors. A total of 30 features were used. Included in these features are subtractions of color components of different color spaces. The results showed that the neural network classifier was obtained with a group of 5 features. Another key point was the separation of sputum smear microscopy images in two groups: the first one presenting a high-density background and the second one presenting a low-density background. The precision obtained with images of LDB group was 99.1%, while the precision obtained with images of HDB group was 92.8. The overall sensitivity obtained was 91.53%, while the false detection was 8.51%. Khutlang et al. [7] reported a sensitivity of 97.77%, but not included bacilli with V shape in the counting. Sotaquira et al. [6] reported a false detection of 9.78%.

TABLE IV
PERFORMANCE OF THE BEST PIXEL CLASSIFIERS

Classifier	Sample	Accuracy (%)	Sens. (%)	Spec. (%)
Neural Network	Train	90.87	92.75	89.00
	Test	91.45	93.41	89.50

TABLE V
PERFORMANCE OF THE CLASSIFIERS IN BACILLI SEGMENTATION

Classifier	Group	Sensitivity (%)	Precision (%)	False detection (%)
Neural network	HDB	94.16	50.63	49.37
	LDB	90.32	94.78	5.22
	All images	92.47	63.36	36.64

TABLE VI
PERFORMANCE AFTER ECCENTRICITY FILTER APPLICATION

Classifier	Group	Sensitivity (%)	Precision (%)	False detection (%)
Neural network	HDB	93.22	70.53	29.47
	LDB	89.40	97.39	2.61
	All images	91.53	80.06	19.94

TABLE VII
PERFORMANCE AFTER COLOR RATIO FILTER APPLICATION

Classifier	Group	Sensitivity (%)	Precision (%)	False detection (%)
Neural network	HDB	93.22	92.8	7.2
	LDB	89.40	99.1	0.9
	All images	91.53	91.49	8.51

ACKNOWLEDGMENTS

We would like to thank FAPEAM/FINEP and CNPq (process 470972/2011-4), for financial support and the company FabriQ for the partial release of student Clahildek Matos Xavier. AcademicEnglishSolutions.com

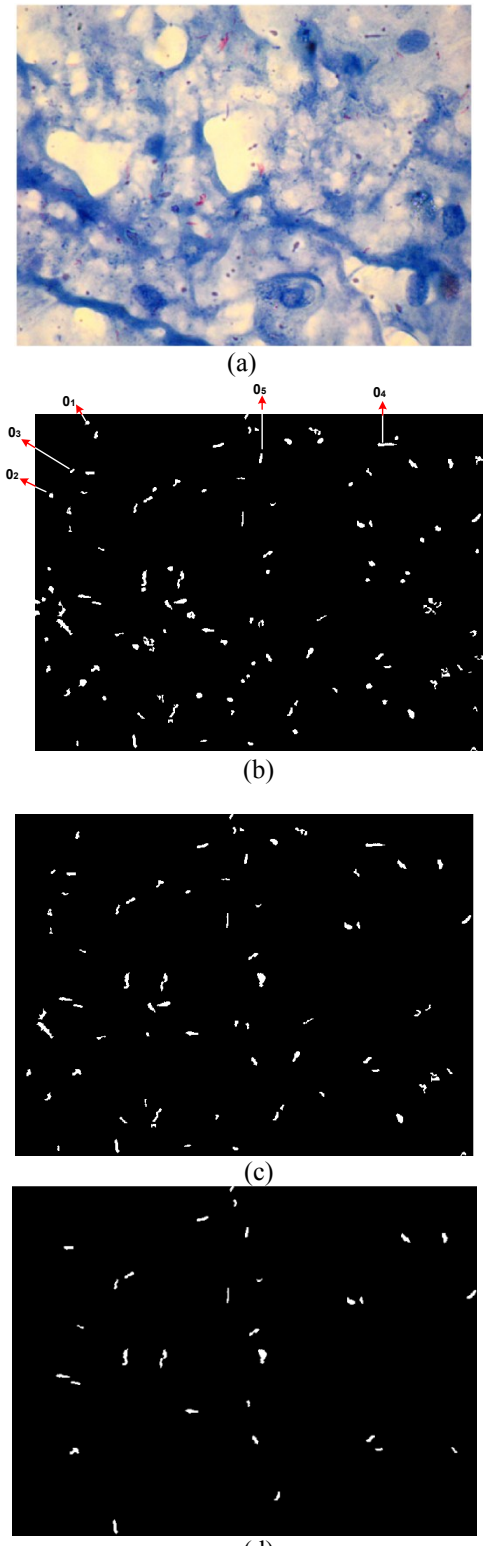

Fig. 5: (a) original image; (b) output of segmentation; (c) output of eccentricity filter; (d) output of color ratio filter.

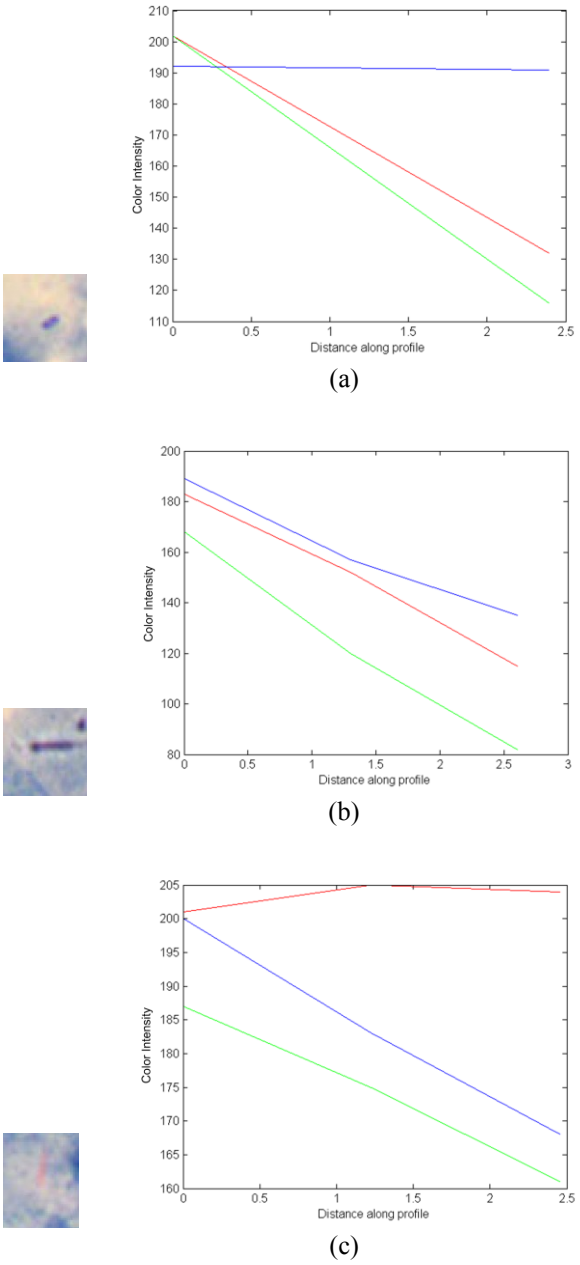

Fig. 6: (a) object O_3 with corresponding profile RGB; (b) object O_4 with corresponding profile RGB; (c) object O_5 with corresponding profile RGB

REFERENCES

[1] World Health Organization (2011) Facts sheets on tuberculosis. [Online]. Available: http://www.who.int/tb/publications/2011/factsheet_tb_2011.pdf

[2] J. Bennedsen, S. O. Larsen, "Examination for tubercle bacilli by fluorescence", Scandinavian Journal of Respiratory Disease, Vol. 47, pp.114–20, 1966.

[3] K. R. Steingart, M. Henry, P.C. Hopewell, A. Ramsay, J. Cunningham, R. Urbanczik, M. Perkins, M. A. Aziz, M. Pai, "Fluorescence versus conventional sputum smear microscopy for tuberculosis: a systematic review", Lancet Infectious Diseases, Vol. 6, pp. 570-581, 2006.

[4] K.Toman, "What are the advantages and disadvantages of fluorescence microscopy?" In: Toman's Tuberculosis Case detection,

treatment, and monitoring –questions and answers, T. Frieden, pp. 7-10, World Health Organization, Hong Kong, China, 2004.

[5] M. G. Forero, G. Cristóbal, M. Desco, "Automatic identification of Mycobacterium tuberculosis by Gaussian mixture models", Journal of Microscopy, Vol. 223, pp. 120–132, 2006.

[6] M. Sotaquirá, L. Rueda, R. Narvaez, "Detection and quantification of bacilli and clusters present in sputum smear samples: a novel algorithm for pulmonary tuberculosis diagnosis", Proceedings of International Conference on Digital Image Processing, Bangkok, Thailand, pp. 117-121, 2009.

[7] R. Khutlang, S. Krishnan, R. Dendere, A. Whitelaw, K. Veropoulos, G. Learmonth, T. S. Douglas, "Classification of Mycobacterium tuberculosis in Images of ZN-Stained Sputum Smears", IEEE Transactions on Information Technology in Biomedicine, Vol. 14, No. 4, pp. 949-957, 2010.

[8] K. Veropoulos, C. Campbell, G. Learmonth, B. Knight, J. Simpson, "The Automated Identification of Tubercle Bacilli using Image Processing and Neural Computing Techniques", Proceedings of 8th International Conference on Artificial Neural Networks, Vol. 2, pp. 797-802, 1998.

[9] M. G. Forero, F. Sroubek, G. Cristóbal, "Identification of tuberculosis bacteria based on shape and color", Real Time Imaging, Vol. 10, pp. 251–262, 2004.

[10] A. Kimura, M.G. Costa, C.F. Costa Filho, L.B.M. Fujimoto and J. Salem, "Evaluation of autofocus functions of conventional sputum smear microscopy for tuberculosis," 32th Annual International Conference of the IEEE EMBS Buenos Aires, Argentina, Aug. 31 – Sept. 4, 2010.

[11] S. Theodoridis and K. Koutroumbas, *Pattern Recognition*, 3th ed., Ed. Elsevier Academic Press, 2009.

[12] A. Cichoki, R. Unbehauen, Neural Networks for Optimization and Signal Processing, 2003.

[13] F. L de A. Andrade, Graduation Thesis, Computer Engineering Course, Federal University of Amazonas, 2011.